COMPDYN 2015
5th ECCOMAS Thematic Conference on
Computational Methods in Structural Dynamics and Earthquake Engineering
M. Papadrakakis, V. Papadopoulos, V. Plevris (eds.)
Crete Island, Greece, 25–27 May 2015

INFLUENCE OF JOINT RESPONSE IN THE ASSESSMENT OF SEISMIC PERFORMANCE OF EXISTING REINFORCED CONCRETE FRAMES

Maria Teresa De Risi[1], Paolo Ricci[1], and Gerardo M. Verderame[1]

[1] University of Naples Federico II – Department of Structures for Engineering and Architecture
via Claudio 21, Naples
e-mail: mariateresa.derisi@unina.it, paolo.ricci@unina.it, verderam@unina.it

Keywords: Earthquake Engineering, Seismic Performance, Reinforced Concrete Frames, Beam-Column Joints.

Abstract. *In the seismic performance assessment of existing Reinforced Concrete buildings, non-ductile failures related to beam-column joint regions can represent a critical issue. Therefore, within the context of Performance-Based Earthquake Engineering, a growing attention should be addressed to the behavior of these non-ductile elements, starting from the classification of their failure typology.*
In particular, in typical existing buildings, seismic performance might be significantly affected by the non-linear behavior of joints which are involved in the failure mechanisms because of poor structural detailing (e.g. lack of an adequate transverse reinforcement in joint panel, deficiencies in the anchorage or absence of any capacity design principle). Nevertheless, conventional modeling approaches consider only beam and column flexibility, although joints can provide a great contribution to the global deformability.
In this study, a numerical investigation on the influence of joint response on the seismic behavior of a case study RC frame – designed for seismic loads according to an obsolete technical code – is performed. A preliminary classification of joint failure typology of the elements within the frames and the definition of the corresponding nonlinear behavior are carried out. Structural models that explicitly include beam-column joints are built. A probabilistic assessment based on nonlinear dynamic simulations of structural behavior is performed to evaluate the seismic response at different performance levels. Uncertainty in seismic ground-motion is accounted for.

1 INTRODUCTION

Assessment of seismic performance of structures requires the development of nonlinear analysis models that can detect all possible local and global collapse modes.

Potential element deterioration and failure modes are a consequence of the design and detailing requirements, materials properties and structural system. Thus, once all failure typologies have been identified for a given structural system, the attention can be focused on a subset of likely collapse mechanisms by means of the analysis of experimental test data, engineering judgment, analytical models, and observations of damage from past earthquakes. The identified collapse modes then serve as the basis for selecting appropriate simulation and damage models that can be used to predict structural seismic performance.

The building code requirements for modern moment-resisting frames are designed to promote ductile and more desirable collapse modes, preventing the formation of the brittle collapse modes ([1]-[3]): the strong column – weak beam requirement promotes flexural hinging in beams before columns; likewise, shear strength capacity design provisions for beams and columns should ensure that shear failure is highly unlikely in beam-column elements. Vice-versa, older RC moment-resisting frames, with minimal detailing requirements used in their design, are vulnerable to a wider range of possible collapse modes ([4]-[7]). These structures have a demonstrated tendency to fail in soft story or column-hinging mechanisms [8], when they are designed for gravity loads only, or to exhibit joint failures [9], also if old seismic codes are adopted for the design [10]. Less stringent detailing requirements may also promote lap-splice failure or pull-out of the bottom beam reinforcing bars anchored into the joint panel. Moreover, column shear failure may occur, depending on the column's design and gravity loading [11].

Therefore, in seismic performance assessment of non-conforming RC buildings, non-ductile failures related to beam-column joint regions and their modeling may represent a critical issue.

In this study, a numerical investigation on the influence of joint failures on the seismic performance at different performance levels of a case study RC frame - designed for seismic loads according to an obsolete technical code - is performed. A preliminary classification of joint failure typology within the frames and the definition of the corresponding nonlinear behavior are carried out. Structural models that explicitly include beam-column joints are built. In particular, the empirical model proposed by the Authors [12] for exterior joints was applied, in conjunction with modeling proposals from literature for interior joints [9] and beam/column behavior [13], as explained in Section 2.

A probabilistic assessment based on nonlinear dynamic simulations of the structural response is performed taking into account record-to-record variability.

2 STRUCTURAL MODELING

Analytical evaluation of seismic performance at different performance levels requires primarily the accurate modeling of nonlinear behavior and deterioration due to seismic loading for each of the constituent element in the structural system, such that all possible local and global collapse modes can be captured. Therefore, to ensure that the model faithfully represents the structure and its possible failure modes, an accurate representation of material properties and deterioration of beam/column elements and joints is needed.

An overview of the frame modeling adopted in this study is shown in Figure 1.

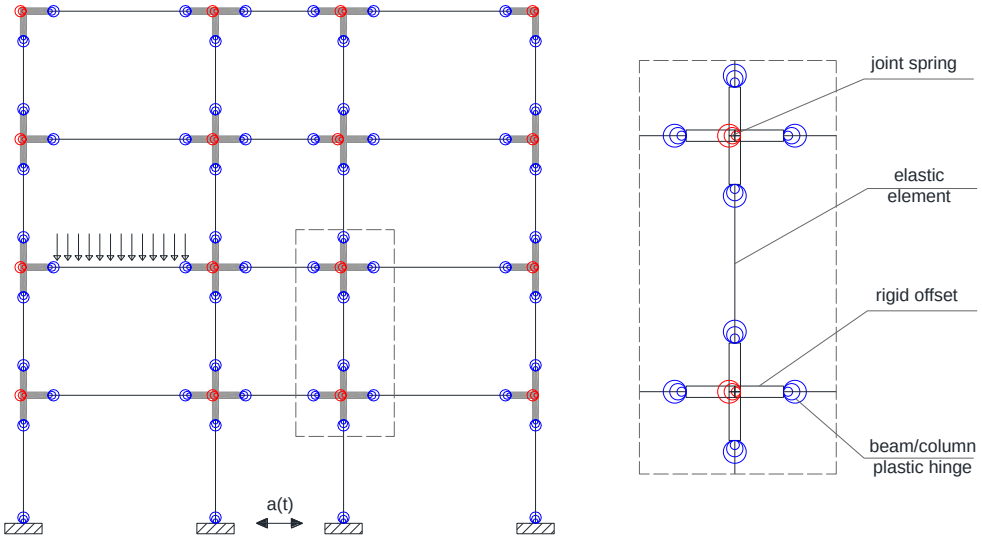

Figure 1: Adopted structural model.

Nonlinear element models for RC beams/columns developed by Ibarra, Medina, and Krawinkler [14] and calibrated by Haselton et al. [13] is adopted in this study to capture the yielding, strain hardening, and spalling and rebar buckling that lead to degradation of strength and stiffness in the structure. The database adopted for the calibration by [13] includes RC columns with both ductile and non-ductile detailing, and varying levels of axial load and geometries. Approximately 35 of the 255 column tests have non-ductile detailing and failed in flexure-shear, as expected for the older RC columns of interest in this study. However, the model cannot capture explicitly the onset of shear failure with the subsequent axial collapse of column, because the column model does not incorporate axial-shear interaction.

Lumped plasticity models also account for bond-slip that occurs in regions of high bond stresses in beam-column joints. Also rebar pull-out and the resulting loss in strength could be accounted for by introducing an additional spring, properly defined as a function of bond stress-slip relationship and anchorage length. However, in the case study analyzed herein, the latter possible failure is excluded, by assuming that a sufficient anchorage length or efficient anchorage devices are guaranteed, as common construction practice provided for, especially for seismic designed structures.

It is worth noting that the simulation model is not able to capture all possible collapse modes, in particular the onset of columns shear failures and the subsequent degrading behavior. To develop flexural behavior, the member shear strength must be larger than the flexural strength, which is the condition typically required in capacity design provisions for seismic design. Where the shear strength is not sufficient to preclude shear failure (such as in most of the existing buildings), shear effects must be considered in the analysis model in addition to flexural and axial load effects. Nevertheless, modeling the cyclic response of a RC element experiencing shear deterioration is complex due to the interactions of shear, moment, and axial forces, as well as the overall brittle nature of this deterioration mode. A review of previous researches on the shear behavior of existing columns [15] have indicated that it is quite difficult that column shear models satisfy all the needed requirements of accuracy, computationally efficiency and compatibility with existing software programs. The problem is still an open and important issue, but, in the present work, shear failures are not accounted for.

Modeling of joint shear behavior in beam-column joints is the focus of Section 2.1.

2.1 Joints modeling

Two main different modes of joint failure can be identified (if no anchorage failure of longitudinal reinforcement anchored into the joint panel occurs, as in the case analyzed in this study): (i) joint shear failure prior to (J-failure) or after than (BJ-failure) yielding of beam longitudinal reinforcement (in hypothesis of strong column-weak beam). In both cases, to capture nonlinear behavior and deterioration associated with degradation of shear strength and stiffness in the beam-column joint regions, the shear panel is modeled with an inelastic rotational spring and rigid offsets spreading into the joint panel, namely by means of the so-called scissors model [16].

In literature there are several models available to reproduce joint shear behavior into numerical analyses of RC frames, basically lumped plasticity approaches, multi-spring macromodels or finite element simulations. It can be pointed out that finite element models are too demanding in terms of computational efforts for a great number of analyses, while models with multiple nodes and multiple springs (e.g. [17]-[19]) require more limited computational efforts allowing to capture realistically the joint panel kinematic behavior and simulate the horizontal translation that can occur between the centerlines of the columns above and below the joint. Vice-versa, the scissors model by Alath and Kunnath [16] does not capture this possible kinematic response, but it is the simplest and computationally less demanding joint model and it seems to be sufficiently accurate in predicting the experimental beam-column joint panel response for simulating the seismic response of non-conforming RC frames for purposes of fragility assessment and performance-based earthquake engineering [9].

Therefore, both for exterior and interior joints, the scissors model has been adopted. No springs at the interface between the joint panel and the adjacent beams/columns representing the bond-slip contribution are introduced in these analyses because the deformability contribution due to bond slip is already accounted for in beam/column rotational springs.

The joint panel model adopted herein is implemented by defining duplicate nodes, node A (master) and node B (slave), with the same coordinates at the center of the joint panel. Node A is connected to the column rigid link and node B is connected to the beam rigid link. A zero length rotational spring connects the two nodes and allows only relative rotation between them through a constitutive model which describes the shear deformation of the joint panel zone, and that is different for exterior and interior joints. In both cases, such a rotational spring is defined as a quadri-linear moment (M_j) – rotation (γ_j) spring characterized by four characteristic points (Figure 2): cracking, pre-peak, peak and residual points.

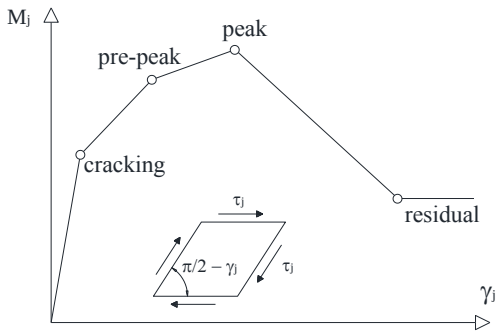

Figure 2: Schematic stress-strain relationship for the rotational spring representing joint panel.

In particular, in this study, the model approach proposed by the Authors [12] is adopted for exterior joints. The proposed model provides only a backbone for the joint moment-rotation

relationship. The calibration of the relative cyclic behavior, that is essential to perform dynamic nonlinear analyses, is carried out herein including cyclic degradation in unloading and reloading stiffness and pinching effects.

Exterior joints

The joint panel zone model for exterior unreinforced joints was calibrated through tests well documented in literature, different for the failure mode they exhibited, namely J-failure (by [20] – here referred to as Pant2, Pant3, Pant5, Pante6) and BJ-failure (by [21] – here referred to as Clyde2, Clyde4, Clyde5, Clyde6), for which experimental shear stress-strain relationships for joint panel were available.

Key parameters defining the quadri-linear backbone of the proposed joint rotational spring for exterior joints are reported in details in [12] and [15] and briefly summarized in Table 1, in terms of shear stress (τ_j) – versus shear strain (γ_j), separately for J- and BJ-mode of failure. From simple equilibrium equation, for each characteristic point of the backbone, the moment transferred through the rotational spring M_j can be obtained as a function of the joint shear stress τ_j.

Backbone point	**J-failure**		**BJ-failure**	
	τ_j	γ_j	τ_j	γ_j
cracking	from [22]	0.06%	from [22]	0.06%
pre-peak	0.9 τ_{peak}	0.21%	τ ($M_{yielding,beam}$)	0.26%
peak	from [23]	0.48%	from [23]	0.63%
residual	0.6 τ_{peak}	2.86%	0.7 τ_{peak}	3.03%

Table 1: Summary of the proposed backbone for the joint panel.

The same tests adopted for the calibration of the backbone described above are considered to calibrate the cyclic behavior of the joint shear stress-strain response of this typology of joints. The calibration is performed in OpenSees ([24]) on the basis of the hysteresis rules characterizing the *Pinching4* material, so that the obtained parameters can be practically employed in modeling of RC frames. Pinching4 material is a four-points uniaxial material developed by Lowes et al. ([25]) and belonging to the library of OpenSees, that allows to model the cyclic degradation of unloading and reloading stiffness (through the parameters gk and gD, respectively), degradation in strength (through the parameters gF) and pinching effects (through the parameters rDisp, rForce and uForce). Calibration of these key parameters was performed starting from the experimental shear stress-strain backbones and minimizing the error in terms of energy dissipated between the numerical and the experimental responses. No degradation in strength was introduced since it is already included in the backbone of the joint response obtained from experimental data.

In Figure 3 two examples of the comparison between numerical and experimental cyclic responses are presented: experimental backbone and cyclic response are reported in red and grey, respectively; while numerical cyclic response is reported in black. The graphical numerical versus experimental comparison for each of the eight tests is reported in [15].

Table 2 presents the modeling parameters of the Pinching4 material (in positive "P" and negative "N" loading directions) adopted to obtain a good fit of the experimental response of the analyzed non-ductile exterior beam-column joints. The mean value of these parameters will be utilized in structural analyses for a probabilistic performance assessment.

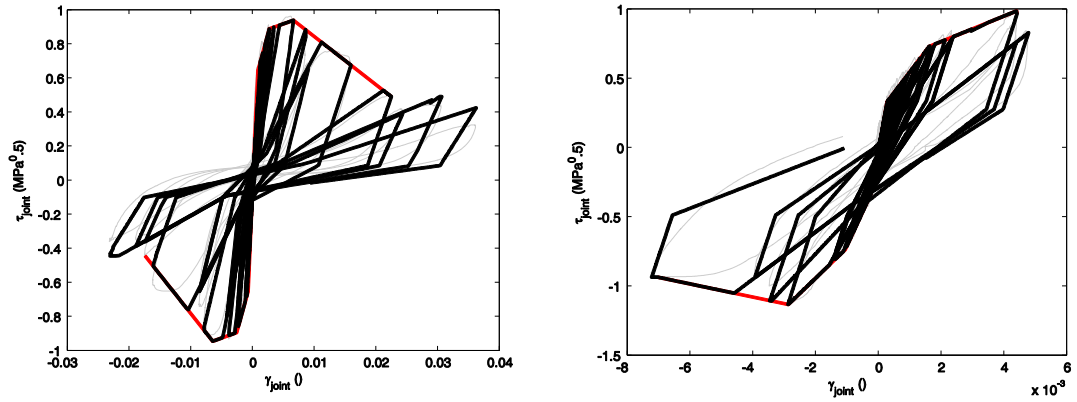

(a) (b)

Figure 3: Cyclic behavior calibration for tests by Pantelides et al. (2002) [20] – Pantelides6 (a) and Clyde et al. (2000) [21] – Clyde6 (b).

	Pant2	Pant3	Pant6	Pant5	Clyde2	Clyde4	Clyde5	Clyde6	Mean	Adopted
rDisp P	0.2	0.2	0.2	0.2	0.1	0.2	0.2	0.2	0.19	0.16
rDisp N	0.2	0.2	0.2	0.2	-0.1	0.2	-0.1	0.3	0.14	
rForce P	0.2	0.2	0.2	0.2	0.2	0.2	0.2	0.2	0.20	0.23
rForce N	0.2	0.2	0.2	0.2	0.2	0.2	0.4	0.4	0.25	
uForce P	-0.2	-0.2	-0.2	-0.05	-0.05	-0.25	-0.2	-0.5	-0.21	-0.22
uForce N	-0.2	-0.2	-0.2	-0.2	-0.2	-0.2	-0.2	-0.4	-0.23	
gK1	0.9	0.9	0.9	0.8	0.9	0.95	0.95	0.5	0.85	0.85
gK3	0.1	0.1	0.1	0.1	0.1	0.2	0.15	0.1	0.12	0.12
gKlim	0.95	0.95	0.95	0.95	0.95	0.99	0.95	0.95	0.96	0.96
gD1	0.35	0.35	0.35	0.35	0.25	0.35	0.6	0.4	0.38	0.38
gD3	0.15	0.15	0.15	0.15	0.15	0.15	0.9	0.9	0.34	0.34
gDlim	0.95	0.95	0.95	0.95	0.95	0.95	0.99	0.99	0.96	0.96

gF1= gF2= gF3= gF4= gFlim=0; gK2=gK4=0; gD2=gD4=0.

Table 2: Parameters adopted to reproduce the hysteretic behavior of exterior unreinforced joints in Pinching4 material.

Interior joints

The joint moment-rotation constitutive relationship proposed by Celik and Ellingwood [9], within the modeling approach of the scissors model, is adopted in this study for interior joints. This relationship was based on a statistical analysis carried out on the basis of experimental tests.

Celik and Ellingwood also suggested that the shear stress-strain backbone curve for the panel zone in typical non-conforming RC beam-column joints can be defined through four key points, which correspond to joint shear cracking, reinforcement yielding, joint shear strength or contemporary achievement of adjoining beam or column capacity, and residual joint strength, respectively. The ordinates of the backbone points were reduced if the shear failure of the joint occurs before beams or columns reach their capacities. Shear failure of the joint is assumed to depend on the kind of joint (interior/exterior) and the anchorage conditions.

In particular, the abscissas of the four key points $\gamma_{j,cr}$, $\gamma_{j,y}$, $\gamma_{j,max}$, $\gamma_{j,res}$, typicalIy fall within the following ranges: 0.0001-0.0013, 0.002-0.010, 0.01-0.03, and 0.03-0.10 radians, respectively. Joint shear strength $\tau_{j,max}$ is proposed in analogy with ASCE-SEI/41 prescription and it falls within the range 0.75-1.00 $(MPa)^{0.5}$ for interior beam-column joints. Residual strength is

assumed equal to shear stress corresponding to joint cracking (evaluated by means of Uzumeri formulation [22]). Mean values of the proposed ranges are adopted in this study, since modeling uncertainties are not considered in structural analyses herein.

The proposal by Celik and Ellingwood also included joint moment-rotation constitutive relationship for exterior joints. However, from the analysis of the experimental dataset they adopted, it was observed that the proposed joint shear strain values for the four key points are related to interior joints tests only; such values are very high if compared with shear strain values obtained from experimental tests on exterior beam-column joints. Therefore, the proposal by Celik and Ellingwood is adopted for interior joints only.

In the proposal by Celik and Ellingwood [9], anchorage failure was also taken into account through a reduced envelope for the joint shear stress-strain relationship. However, in this study, no reduction of joint shear stress is considered, since the hypothesis that a sufficient anchorage length or efficient anchorage devices are guaranteed, thus excluding this failure mode.

By proposing that joint strength should be assumed as the minimum between empirical shear strength and the maximum joint shear stress related to beam/column flexural capacity, this model is the only one able to reproduce the softening response of the joint panel also when a BJ-failure occurs. This is in accordance with the modeling adopted for exterior joints (since the nature of the strength model by [23] adopted for exterior joints) and with observed experimental results [26], which showed that beam-column intersections always exhibited a degradation response if joint cracking was occurred.

Furthermore, since the proposal by Celik and Ellingwood suggests only pinching parameters to model joints hysteretic response, the parameters calibrated by Jeon et al. [10] for the Pinching4 material in OpenSees for the hysteretic response of interior joints are adopted herein. However, these parameters are modified so that no strength degradation was taken into account (since strength degradation is already included in the backbone of the joint response obtained from experimental data).

It is worth noting that, in order to reproduce the softening response of the joint when a BJ-failure occurs - as observed experimentally (e.g. [26]) – also for interior joints, the adjacent beams have to be modeled with no post-peak strength degradation. In fact, in the case of BJ failure, the peak strength of interior joints is defined as the maximum shear stress corresponding to the contemporary achievement of flexural capacity in both the adjacent beams. If beam response degrades after its peak is reached, it is highly unlikely that this condition can be achieved during the analysis thus leading the interior joint to go through its softening branch. Since the adjacent beams are in series with the joint panel spring, it was necessary to model the response of the beams as perfectly-plastic after the peak strength is reached. In this way, the contemporary achievement of peak strength in the adjacent beams can be obtained and thus the joint can reach its peak strength, then starting to degrade. For the same reasons, no degradation in strength should be modeled in beams.

This simulation model is not able to capture axial failure in beam-column joints. Therefore, both for exterior and interior joints, this non-simulated failure mode is detected in this study by post-processing dynamic analyses results. Such an approach is adopted because of the lack of experimental data and reliable models that allow capturing this failure mode explicitly in numerical modeling. Unfortunately, very few unconfined joint tests are available with confirmed axial failure, since, generally, during laboratory tests, a common practice has been to terminate the test after dropping to 80% of lateral load resistance without testing the axial capacity of the joint.

In this study, the empirical shear-friction capacity model proposed by Hassan and Moehle [27] calibrated on the basis of available experimental data is adopted. The expression of the IDR threshold (IDR_{AxJ}) that identifies the onset of joint axial failure is reported in Eq. (1):

$$IDR_{AxJ} = 0.057 \cdot \left(\frac{P \cdot tg\theta}{A_{sb} \cdot f_{yb}} \right)^{-0.5} \quad (1)$$

where P is the axial load acting on the joint, A_{sb} and f_{yb} are longitudinal reinforcement area and strength, respectively, of the bottom beam bars, and θ represents the shear critical angle, as reported in [27].

3 CASE STUDY FRAME

A symmetric four-story three-bay frame is designed, modeled as explained in Section 2, and assessed. This case-study frame is the internal frame of a structure with 5 m-transverse bay. Figure 4 represents frontal and in-plane views of the analyzed frame.

Dead load from slab is equal to 5 kN/m^2 for the last story and 7 kN/m^2 for all of the other ones; live load is equal to 1 kN/m^2 for the last story and 2 kN/m^2 for all of the other ones.

The case-study frame (referred to as OLD SLD) is intended to be realized in 1980s and it is designed by means of a simulated procedure according to an obsolete technical code [28] in force in Italy until 1990s, by means of the allowable tensile stress method. The structure is located in a first-category site, corresponding to a design horizontal peak ground acceleration equal to 0.1g. Element dimensions are calculated according to the allowable stresses method; the design value for maximum concrete compressive stress is assumed equal to 6.0 and 8.5 MPa for axial load (σ_c) and axial load combined with bending ($\sigma_{c,f}$), respectively. Reinforcing bars (FeB38K) are deformed and their allowable design stress (σ_s) is assumed equal to 220 MPa.

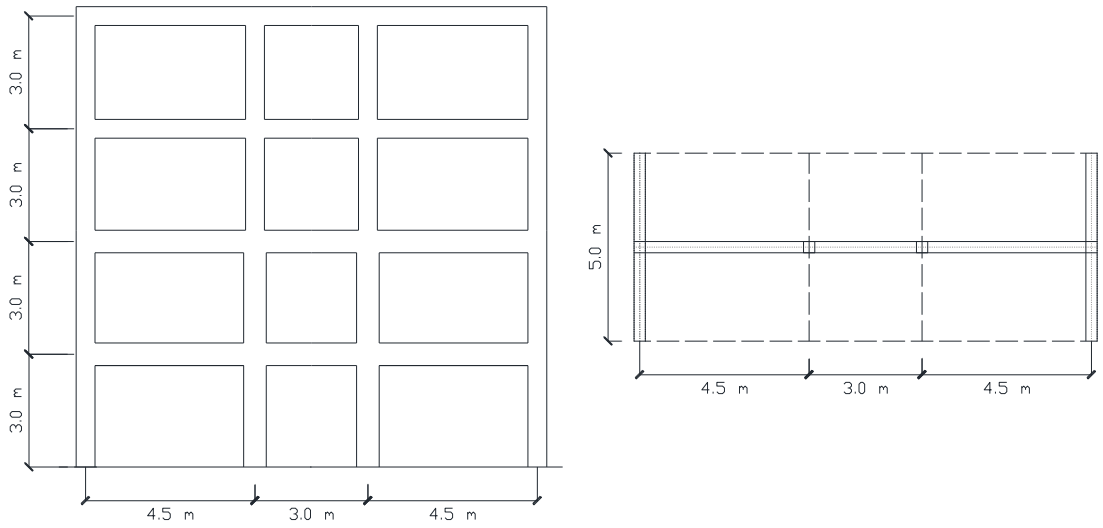

(a) (b)

Figure 4: Case-study frame: frontal (a) and in plane (b) views.

Section dimensions are (30x50) cm^2 for beams and columns of the third and fourth levels, and (30x60) cm^2 for beams and columns belonging to the first and the second levels.

Longitudinal reinforcement ratio ranges between 2 and 2.5% in columns, whereas longitudinal reinforcement at the end sections of beams varies from 0.75 and 0.9% of the section area

for the top layer, and from 0.34 and 0.4% of the section area for the bottom layer. Stirrups spacing in columns was defined as the minimum amount of transverse reinforcement required by the adopted code, namely ϕ8/240 mm in this case.

Expected values of concrete compressive strength (f_c), and steel yielding strength for longitudinal and transverse reinforcement (f_y) adopted in the assessment phase are 20 MPa and 450 MPa, respectively.

In Table 3, it is shown that column-to-beam flexural capacity (M_c/M_b) is significantly higher than the unity; therefore, strong column-weak beam hierarchy characterizes this frame. By reporting beam flexural capacity to the joint centerline ($M_{j,b}$) and by comparing $M_{j,b}$ and joint moment strength ($M_{j,R}$), it can be observed that prevalently J-failures characterize this frame. $M_{j,R}/M_{j,b}$ is equal to the unity when joint strength is limited to the flexural capacity of the adjacent beams, according to the modeling approach described in Section 2.

story	joint	M_b (kNm)	M_c (kNm)	M_c/M_b ()	$M_{j,R}$ (kNm)	$M_{j,b}$ (kNm)	$M_{j,R}$ / $M_{j,b}$ ()	failure mode
1	ext	376.52	1028.46	2.73	384.12	434.45	0.88	J
	int	582.46	1112.56	1.91	528.27	693.41	0.76	J
2	ext	376.52	896.44	2.38	358.46	434.45	0.83	J
	int	582.46	950.81	1.63	423.42	693.41	0.61	J
3	ext	306.29	767.83	2.51	294.69	344.57	0.86	J
	int	473.82	794.07	1.68	333.49	546.71	0.61	J
4	ext	186.16	375.61	2.02	209.43	209.43	1.00	BJ
	int	281.37	383.27	1.36	324.66	324.66	1.00	BJ

Table 3: Beam/column hierarchy and joints classification.

4 PERFORMANCE LEVELS AND GROUND MOTION RECORDS

In order to perform dynamic analyses, input ground motion records have to be selected and performance levels of interest should be identified.

In this study, natural records representing Italian seismicity are selected and scaled to different levels of seismicity. The records selection has been performed by using REXEL software [29], from ITACA strong-motion database. Earthquakes characterized by a low-medium magnitude levels (between 4.4 and 5.7), with a source-to-site distance ranging between 10 and 40 km, and recorded on soil class B are selected. On the whole 50 ground motion records are selected.

As far as performance levels of interest are concerned, the structural capacities are primarily defined by the maximum interstorey drifts (IDR) that correspond to three widely used performance levels (or limit states) in the earthquake community (e.g. [30]): immediate occupancy (IO), life safety or significant damage (SD), and collapse prevention (CP). Table 4 reports the values of the IDR thresholds (IDR_{LS}) for the selected performance levels, chosen on the basis of previous literature researches ([30], [31]).

	IO LS	SD LS	CP LS
IDR_{LS}	0.2%	2%	5%

Table 4: IDR thresholds for the selected performance levels.

Additional LSs, defined on the basis of the achievement of characteristic points in the nonlinear response of the primary structural elements, are adopted. In particular the first achieve-

ment of a particular condition or a "conventional failure" is detected, in analogy with the approach of typical European code prescriptions (e.g. [2], [3]), as shown in Figure 5.

For columns, green circles represent a pre-yielding condition; yellow, orange and red circles indicate the achievement of yielding, capping and post-peak rotations, respectively.

For beam-column joints, white circle identifies a pre-cracking condition of joint; while green, yellow, orange and red circles represent the achievements of joint cracking, pre-peak point, peak joint strength, and residual strength, respectively. Such a convention will be adopted in Section 5 when damage states in RC elements are presented. The corresponding LSs will be referred to as summarized in Table 5.

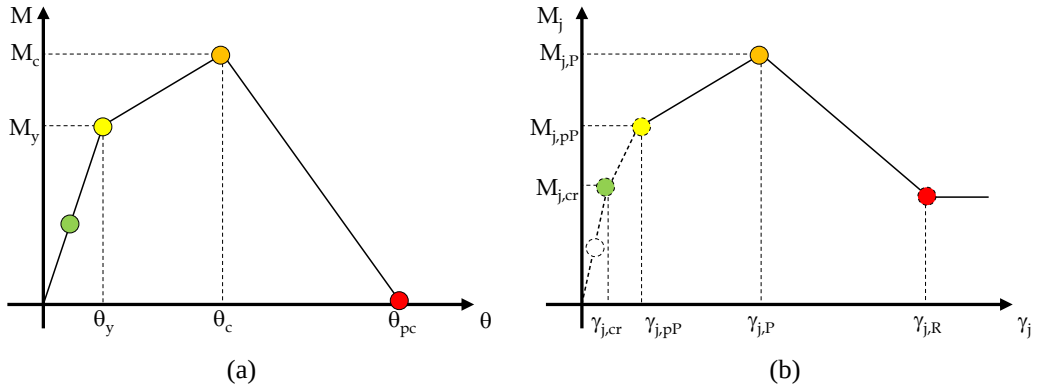

Figure 5: Characteristic points of columns (a) and joints (b) response.

FY	first element at yielding
FC	first element at capping
FPC	first element at post-capping
FcrJ	first joint cracking
FpPJ	first joint at pre-peak point
FPJ	first joint at peak strength
FRJ	first joint at residual strength

Table 5: Additional LSs acronyms.

5 PRELIMINARY NONLINEAR STATIC ANALYSES

Preliminary, nonlinear static analyses with first-mode-shape-proportional lateral load pattern are performed in OpenSees [24] on the structural models (obtained as described in Section 2) in a double condition:

(i) with "rigid joints", assuming a very high stiffness and shear strength for beam-column connections, and

(ii) "with joints", explicitly modeling the nonlinear behavior of joints, as explained in Section 2.1.

Results of this kind of analysis are reported in this Section.

First of all, elastic periods from modal analysis are reported in Table 6 for both conditions ("rigid joints" and "with joints"). An increment of about 8% in elastic period is observed when joint elastic deformability is taken into account.

	Rigid joints	With joints
T_1 (s)	0.694	0.747

Table 6: Elastic periods.

In both cases, for rigid joints condition and when nonlinear response of beam-column joints is modeled, the OLD SLD frame exhibited a global collapse mechanism, as expected due to the strong-column-weak-beam hierarchy observed in Section 3.

Static pushover (SPO) curves and collapse mechanisms and damage levels in each beam/column hinge at the last step are reported in Figure 6 and Figure 7, respectively.

In the case of "rigid joints" no red circle (namely, no beam/column that reach post-peak rotation) is present (see Figure 10a), since SPO was interrupted before the first element reached its post-peak rotation capacity because of a convergence issue. When nonlinear response of beam-column joints is modeled, even if the maximum top displacement at last step is higher with respect to the case of "rigid joints", a lower damage level can be observed in beams (for example at the 2nd and 3rd stories) and a quite distributed damage level in beam-column joints is exhibited, especially from the first to the third story.

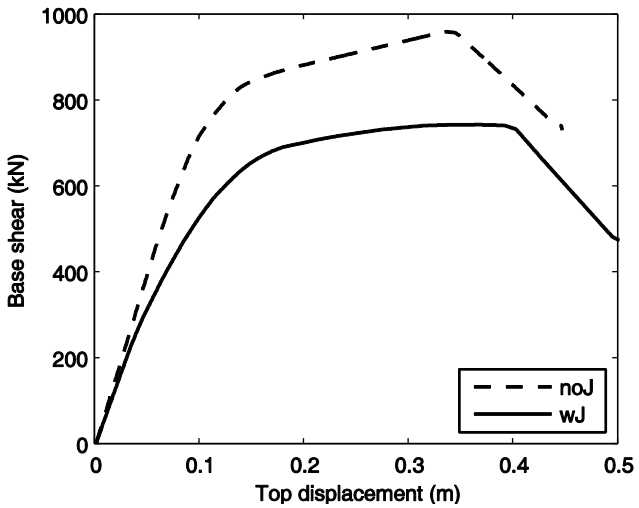

Figure 6: SPO curves: "rigid joints" (noJ) versus "with joints" (wJ).

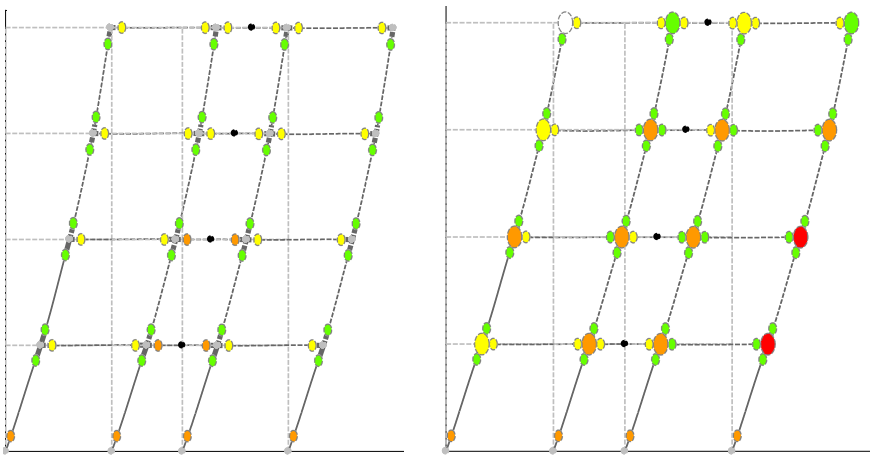

(a) (b)

Figure 7: Collapse mechanism and damage levels at last step: "rigid joints" (a) versus "with joints" (b).

In Table 7, a comparison in terms of peak base shear ($V_{b.max}$) and the corresponding displacement (D_{max}) in SPO analyses "with joint" (wJ) and with "rigid joints" (noJ) is carried out. It can be observed that the explicit modeling of beam-column joints in the structural analysis

implies a reduction of the maximum base shear (equal to 21%) and a slightly higher peak deformability (that increases of about 6%).

	$V_{b,max}$ (kN)	D_{max} (m)	$V_{b,max\ wJ}$/ $V_{b,max\ noJ}$ (-)	D_{wJ}/D_{noJ} (-)
noJ	959.5	0.343	0.79	1.06
wJ	745.2	0.362		

Table 7: Comparison in terms of peak base shear and peak displacement in SPO – "with joint" (wJ) and "rigid joints" (noJ).

6 INCREMENTAL DYNAMIC ANALYSES

The incremental nonlinear dynamic analyses (IDAs) [32] are conducted in OpenSees [24] with the selected ground motion records with "rigid joints" and "with joints".

Robust convergence algorithms for solving simultaneous equations when strength and stiffness are degrading are implemented.

Five percent mass- and tangent stiffness-proportional Rayleigh damping is applied to the first and third mode of elastic response.

First, IDA curves have been obtained and, then, fragility curves have been calculated, at different LSs taking into account only aleatoric uncertainty, namely record-to-record variability. In this study, the structural demand measure is selected to be the maximum interstory drift in the frame, IDR_{max}, which occurs during its dynamic response to earthquake shaking. At lower levels of excitation, the IDR typically provides insight regarding the potential for damage to non-structural components, while at higher levels it is closely related to structural or local collapse. The adopted seismic intensity measure is the spectral acceleration at the fundamental period of the frame, $Sa(T_1)$, for 5% damping, a measure that is consistent with that used in previous studies and that is generally considered as a more efficient parameter to characterize earthquake intensity than peak ground acceleration [33].

In this Section, IDAs and fragility curves at different LSs for the OLD SLD frame are reported and commented. It is worth noting that IDA curves have been scaled to $Sa(T_1)$, where T_1 is the elastic period of the "with joints" configuration, namely 0.747 s.

6.1 Rigid joints

In Figure 8a, IDAs curves related to the "rigid joints" model obtained from all the ground motion records are shown in terms of first-period spectral acceleration $Sa(T_1)$ versus maximum IDR, together with the related median IDA curve.

Starting from such IDAs, fragility curves at LSs defined as the achievement of a given maximum IDR threshold can be easily obtained, by means of a lognormal fit of $Sa(T_1)$ given the value of IDR threshold. In this way, fragility curves shown in Figure 8b have been calculated. Related parameters are reported in Table 8, with μ and β representing the estimated median (expressed in (g)) and logarithmic standard deviation of $Sa(T_1)$ capacity, respectively, at IO, SD, and CP LSs. β-coefficient provides an useful indication about the overall sensitivity of seismic capacity to the variability of the ground motion record, confirming that record-to-record variability is a very important source of uncertainty (β ranges between 41 and 51% for these LSs). Table 8 also reports the maximum IDR threshold (IDR_{max}) corresponding to IO, SD, and CP LSs and the median values ($Sa(T_1)_{median}$) of $Sa(T_1)$, given the maximum IDR.

By means of the same approach based on a lognormal fit of the intensity measure capacities, fragility curves related to the achievement of a certain condition in the elements response for the first time (i.e. in the first element) can be calculated. These fragility curves are report-

ed in Figure 9 and the related parameters in Table 9, where $Sa(T_1)_{median}$ is the median value of $Sa(T_1)$ capacity and IDR_{max} the corresponding median value of maximum IDR.

It can be observed that the yielding condition in the first element (FY LS) occurs for a median value of $Sa(T_1)$ equal to 0.158g, while the achievement of the peak strength for the first time (FC LS) occurs for a quite high value of $Sa(T_1)_{median}$ (1.648g) thanks to the uniform distribution of inelastic demand in the frame. Also in this case, it can be observed that the record-to-record variability provides a logarithmic standard deviation of $Sa(T_1)$ capacity (β) that varies from 42 to 46% for these LSs.

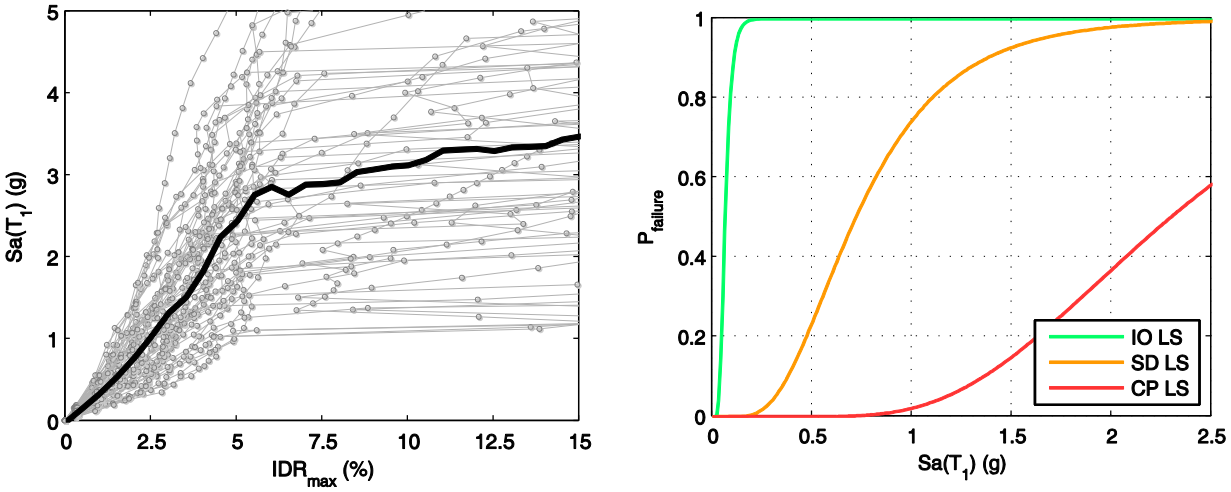

(a) (b)

Figure 8: IDA curves and median IDA (a); fragility curves at IO, SD, and CP LSs (b) – "rigid joints".

LS	$Sa(T_1)_{,median}$ (g)	IDR_{max} (%)	μ (g)	β
IO	0.067	0.20	0.062	0.417
SD	0.783	2.00	0.717	0.506
CP	2.455	5.00	2.293	0.411

Table 8: Fragility parameters at IO, SD, and CP LSs – "rigid joints".

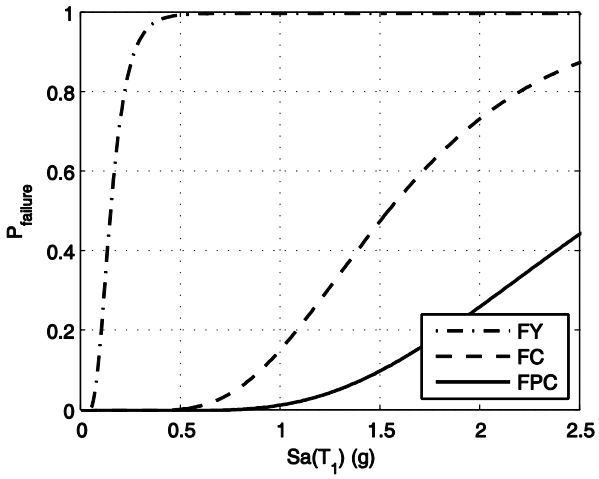

Figure 9: Fragility curves at FY, FC, FPC LSs – "rigid joints".

LS	$Sa(T_1)_{,median}$ (g)	IDR_{max} (%)	μ (g)	β
FY	0.158	0.47	0.145	0.464
FC	1.648	3.71	1.532	0.422
FPC	2.722	5.43	2.656	0.449

Table 9: Fragility parameters at FY, FC, FPC LSs – "rigid joints".

6.2 With joints

The same results are reported also for the structural model that explicitly takes into account joints nonlinear behavior. Figure 10a shows IDAs curves related to the model "with joints" obtained from all the ground motion records, together with the related median IDA curve. Figure 10b reports the fragility curves at IO, SD, and CP LSs, obtained by means of a lognormal fit of $Sa(T_1)$ given the value of IDR threshold for each LS, and Table 10 shows the related parameters.

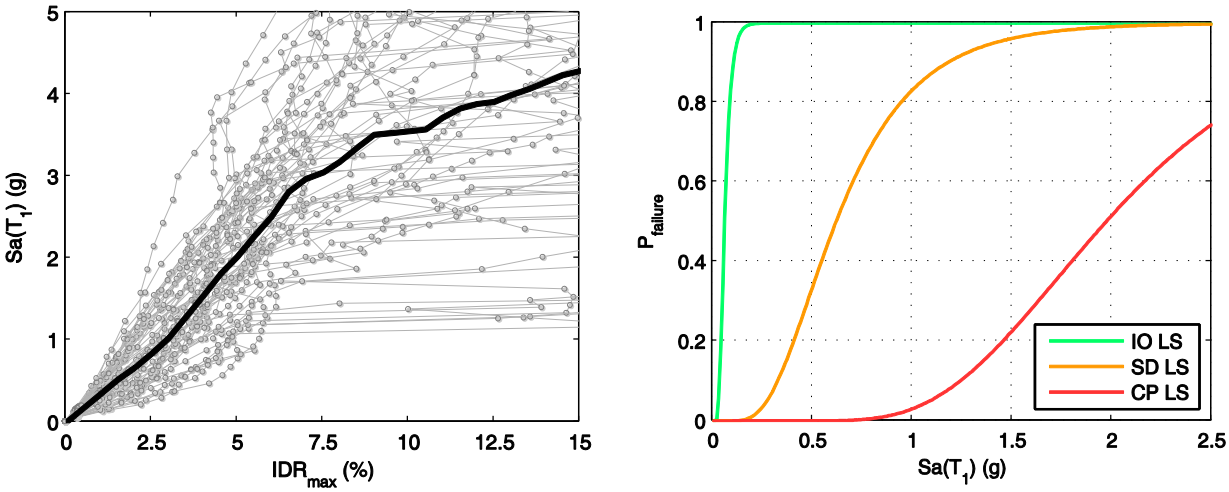

(a) (b)

Figure 10: IDA curves and median IDA (a); fragility curves at IO, SD, and CP LSs (b) – "with joints".

LS	$Sa(T_1)_{,median}$ (g)	IDR_{max} (%)	μ (g)	β
IO	0.070	0.20	0.059	0.432
SD	0.665	2.00	0.617	0.502
CP	2.034	5.00	1.969	0.362

Table 10: Fragility parameters at IO, SD, and CP LSs – "with joints".

Figure 11a and b reports fragility curves obtained in this case at FY, FC, and FPC LSs, but also, at LSs defined as the achievement of particular "limit conditions" in joints response, namely FcrJ, FpPJ, FPJ, and FRJ (defined in Table 5). The related parameters are reported in Table 11, where $Sa(T_1)_{median}$ is the median value of $Sa(T_1)$ capacity and IDR_{max} the corresponding median value of maximum IDR.

It can be observed that the first achievement of peak strength in beam-column joints anticipates the first achievement of capping strength in beams or columns, in terms of $Sa(T_1)_{median}$; the achievement of the peak strength in beams or columns occurs for a value of $Sa(T_1)$ quite

close to that corresponding to the achievement of the first residual strength in joints, thus suggesting that joint damage can be very critical in such a frame, especially for loss estimation.

Moreover, also when joints are explicitly modeled into the numerical model, the possible axial failure of joints cannot be captured directly due to the features of the adopted model. As anticipated in Section 2, a post-processing of the nonlinear analyses can lead to the detection of such kind of failure when the maximum IDR in a story overcomes the minimum IDR capacity (IDR_{AxJ}) among joints at that story. In this way, the achievement of the first axial failure (FAxJ LS) has been detected for each ground motion record and the related fragility parameters has been obtained by means of a lognormal fit (see Table 11 and Figure 11b). A maximum IDR equal to 7.54% leads to the first joint axial failure.

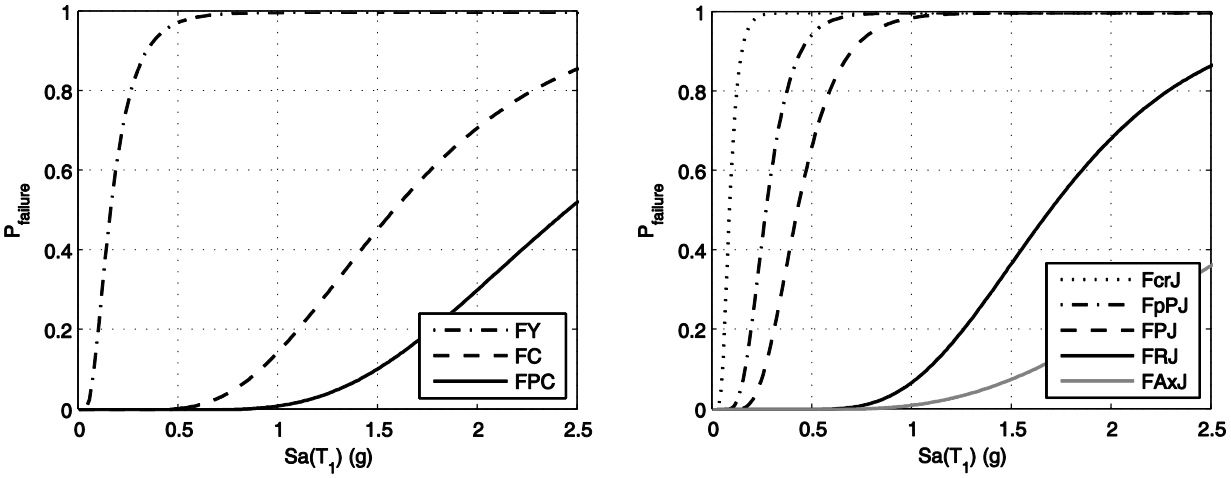

(a) (b)

Figure 11: Fragility curves at FY, FC, FPC LSs (a); Fragility curves at FcrJ, FpPJ, FPJ, FRJ, and FAxJ LSs (b) – "with joints".

DS	$Sa(T_1)_{median}$ (g)	IDR_{max} (%)	μ (g)	β
FY	0.166	0.49	0.157	0.594
FC	1.614	4.14	1.572	0.433
FPC	2.349	5.66	2.441	0.389
FcrJ	0.081	0.24	0.082	0.435
FpPJ	0.296	0.87	0.265	0.394
FPJ	0.470	1.37	0.421	0.385
FRJ	1.706	4.31	1.685	0.354
FAxJ	3.059	7.54	2.947	0.476

Table 11: Fragility parameters at FY, FC, FPC, FcrJ, FpPJ, FPJ, FRJ, and FAxJ LSs – "with joints".

6.3 Comparison

By comparing median IDA curves between the two analyzed frame models ("rigid joints" and "with joints"), as in Figure 12, it can be observed that joint damage leads to lower $Sa(T_1)$ capacity for a given IDR, until about 6% maximum IDR is achieved; successively, when joints involved in the mechanism reach their residual strength - thus starting to go through a constant-strength branch -, IDA curves "with joints" (wJ) keeps increasing, while IDA related to "rigid joints" (noJ) frame goes toward a "flatline".

The difference in $Sa(T_1)$ capacity given IDR that can be observed from the comparison between IDA curves, produces the "distance" between fragility curves that can be observed in Figure 13. The comparison between median $Sa(T_1)$ capacity (from lognormal fitting) with rigid joints (noJ) and with joints (wJ) for the OLD SLD frame is summarized in Table 12 for IO, SD, CP LSs, and also at FY, FC, FPC LSs.

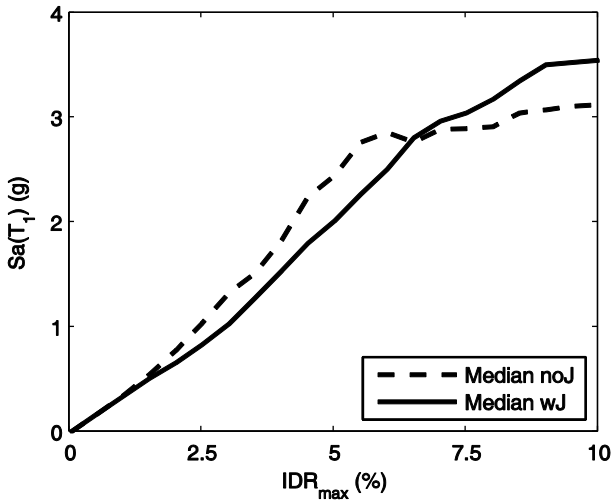

Figure 12: Comparison between median IDA curves.

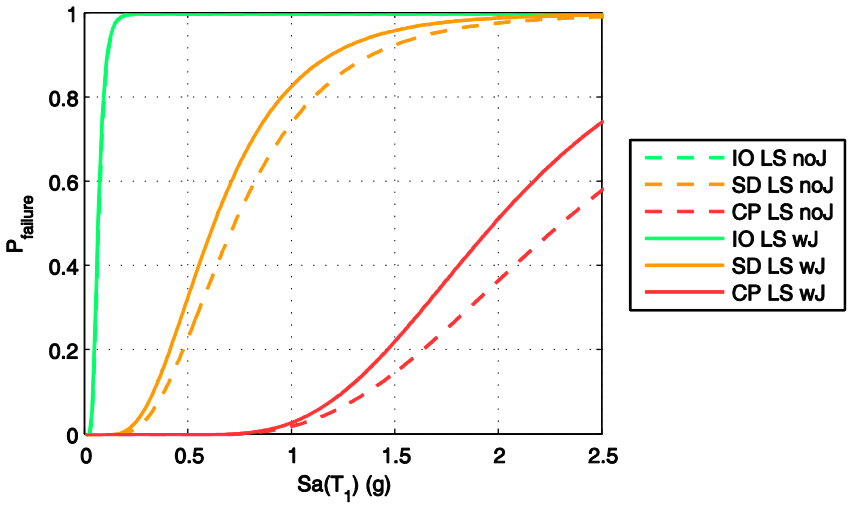

Figure 13: Comparison between fragility curves at IO, SD, and CP LSs.

LS	Sa_{noJ} (g)	Sa_{wJ} (g)	Sa_{wJ}/Sa_{noJ} (-)
IO	0.062	0.059	0.96
SD	0.717	0.617	0.86
CP	2.293	1.969	0.86
FY	0.145	0.157	1.08
FC	1.532	1.572	1.03
FPC	2.656	2.441	0.92

Table 12: Comparison between median $Sa(T_1)$ capacity with rigid joints (noJ) and with joints (wJ).

It can be observed that the minimum ratio between $Sa(T_1)$ capacity with and without nonlinear joint modeling (Sa_{wJ}/Sa_{noJ}) is related to higher seismic intensity, namely at SD, CP and FPC LSs, thus highlighting that the influence of joints in seismic assessment of RC frames becomes more relevant at higher performance levels.

7 CONCLUSIONS

In this paper, a numerical investigation on the influence of joint failures on the seismic performance at different performance levels of a case study RC frame - designed for seismic loads according to an obsolete technical code – has been presented. A preliminary classification of joint failure typology within the frames and the definition of the corresponding nonlinear behavior were carried out. Structural models that explicitly include beam-column joints were built. In particular, the joint model proposed by the Authors has been applied for exterior joints, in conjunction with modeling proposals from literature for interior joints and beam/column behavior. A probabilistic assessment based on nonlinear dynamic simulations of the structural response was performed taking into account record-to-record variability.

The structural capacities were primarily defined by the maximum interstorey drifts (IDR) that correspond to three widely used performance levels in the earthquake community: immediate occupancy, life safety or significant damage, and collapse prevention. Additional LSs, defined on the basis of the achievement of characteristic points in the nonlinear response of the primary structural elements, have been adopted. In particular, the first achievement of a particular condition or a "conventional failure" has been detected, in analogy with the approach of typical European code prescriptions (e.g. Eurocode 8, DM 2008).

Preliminary nonlinear static analyses and incremental nonlinear dynamic analyses under selected ground motion records have been performed in OpenSees in a double condition:

(i) with "rigid joints", assuming a very high stiffness and shear strength for beam-column connections;

(ii) "with joints", explicitly modeling the nonlinear behavior of beam-column intersections.

It was observed that for the analyzed frame (characterized by strong column-weak beam design):

- the minimum ratio between $Sa(T_1)$ capacity with and without nonlinear joint modeling is related to higher seismic intensity levels, thus highlighting that the influence of joints in seismic assessment becomes more relevant at higher performance levels;
- when nonlinear response of beam-column joints is modeled, a lower damage level can be observed in beams/columns and a quite distributed damage level in beam-column joints is exhibited, thus confirming that joint damage can be very critical in such a frame, especially for loss estimation.

Incremental dynamic analysis alone does not account for how well the nonlinear simulation model represents the real frame, since no modeling uncertainties have been considered. These modeling uncertainties are especially important in predicting collapse. Thus, also modeling uncertainties should be accounted for in future works to a more reliable evaluation of seismic performance.

Another important improvement of the study presented herein will be the explicitly modeling of shear failures with degrading behavior after detection and consequent axial failure by means of a reliable, realistic and computational sustainable model.

REFERENCES

[1] ACI. Building Code Requirements for Structural Concrete (ACI 318), 2002.

[2] CEN European standard EN1998-3, Eurocode 8: design provisions for earthquake resistance of structures – Part 3: assessment and retrofitting of buildings. European Committee for Standardisation, Brussels, 2005.

[3] DM 2008, Decreto Ministeriale del 14/1/2008, Approvazione delle nuove norme tecniche per le costruzioni. G.U. n. 29 del 4/2/2008. (in Italian)

[4] L. E. Aycardi, J. Mander and A. Reinhorn, Seismic Resistance of Reinforced Concrete Frame Structures Designed Only for Gravity Loads: Experimental Performance of Subassemblages. *ACI Structural Journal* **91**(5): 552-563, 1994.

[5] S. K.Kunnath, G. Hoffmann A. M. Reinhorn and J. B. Mander, Gravity-Load-Designed Reinforced Concrete Buildings -Part I: Seismic Evaluation of Existing Construction. *ACI Structural Journal* **92**(3): 343-354, 1995.

[6] A.G. El-Attar, R.N. White, P. Gergerly, Behavior of gravity load designed reinforced concrete buildings subjected to earthquakes, *ACI Structural Journal* **94**(2): 133– 145, 1997.

[7] A. Filiatrault, E. Lachapelle and P. La Montagne, Seismic performance of ductile and nominally ductile reinforced concrete moment resisting frames I. Experimental Study. *Canadian Journal of Civil Engineering* **25(**2): 331-341, 1998.

[8] A. B. Liel, Assessing the collapse risk of California's existing reinforced concrete frame structures: Metrics for seismic safety decisions. Diss. Stanford University, 2008.

[9] O.C. Celik and B.R. Ellingwood, Modeling Beam-Column Joints in Fragility Assessment of Gravity Load Designed Reinforced Concrete Frames, *Journal of Earthquake Engineering*. **12:**357-381, 2008.

[10] J. S. Jeon, L. N.Lowes, R. DesRoches, and I. Brilakis, Fragility curves for non-ductile reinforced concrete frames that exhibit different component response mechanisms. *Engineering Structures* **85**: 127-143, 2015.

[11] K. J. Elwood, Modelling failures in existing reinforced concrete columns. *Canadian Journal of Civil Engineering* **31**.5: 846-859, 2004.

[12] M.T. De Risi, P. Ricci, G.M. Verderame, G. Manfredi, A nonlinear macro model of exterior RC joints without transverse reinforcement under seismic load. *Engineering Structures* (submitted), 2015.

[13] C. Haselton, A. Liel, S. L. Taylor and G.G. Deierlein, Beam-Column Element Model Calibrated for Predicting Flexural Response Leading to Global Collapse of RC Frame Buildings, Pacific Earthquake Engineering Research Center 2007/03, University of California at Berkeley, 2007.

[14] L. F. Ibarra, R. A. Medina and H. Krawinkler, Hysteretic Models that Incorporate Strength and Stiffness Deterioration. *Earthquake Engineering and Structural Dynamics* **34**: 1489- 1511, 2005.

[15] M.T. De Risi, Seismic performance assessment of RC buildings accounting for structural and nonstructural elements. Ph.D. Thesis, University of Naples Federico II, Naples, Italy, 2015.

[16] S. Alath, S. K. Kunnath. Modeling inelastic shear deformations in RC beam–column joints. Engineering mechanics proceedings of 10th conference, May 21–24, University of Colorado at Boulder, Boulder, Colorado, vol. 2. New York: ASCE: p. 822–5, 1996.

[17] L.N. Lowes. and A. Altoontash, Modeling Reinforced-Concrete Beam-Column Joints Subjected to Cyclic Loading, *Journal of Structural Engineering*. **129**:1686-1697, 2003.

[18] M. Shin, and J.M. LaFave, Modeling of cyclic joint shear deformation contributions in RC beam-column connections to overall frame behaviour. *Structural Engineering and Mechanics*, **18**(5), 645-669, 2004.

[19] A. Sharma, R. Eligehausen, G. R. Reddy, A new model to simulate joint shear behavior of poorly detailed beam–column connections in RC structures under seismic loads, part I: exterior joints. *Engineering Structures*, **33**(3), 1034-1051, 2011.

[20] C. P. Pantelides, J. Hansen, J. Nadauld, L. D. Reaveley, Assessment of Reinforced Concrete Building Exterior Joints with Substandard Details, PEER Report, No. 2002/18, Pacific Earthquake Engineering Research Center, University of California, Berkeley, USA, 2002.

[21] C. Clyde, C.P. Pantelides, L. D. Reaveley, Performance-Based Evaluation of Exterior Reinforced Concrete Buildings Joints for Seismic Excitation, PEER Report, No. 2000/05, Pacific Earthquake Engineering Research Center, University of California, Berkeley, USA, 2000.

[22] S. M. Uzumeri, Strength and ductility of cast-in-place beam-column joints. *American Concrete Institute Annual Convention, Symposium on Reinforced Concrete Structures in Seismic Zones*, San Francisco, 1974. No. SP-53, 1977.

[23] S. Park and K.M. Mosalam, Analytical model for predicting the shear strength of unreinforced exterior beam-column joints, *ACI Structural Journal* **109**, 149–159, 2012.

[24] F. McKenna, G.L. Fenves, M. H.Scott, OpenSees: Open System for Earthquake Engineering Simulation. Pacific Earthquake Engineering Research Center. University of California, Berkeley, CA, USA. http://opensees.berkeley.edu. Reinforced Concrete Beam-Column Joints, Doctoral Dissertation, Stanford University, 2010.

[25] L. N. Lowes, N. Mitra and A. Altoontash, A Beam-Column Joint Model for Simulating the Earthquake Response of Reinforced Concrete Frames, Pacific Earthquake Engineering Research Center, College of Engineering, University of California, 2004.

[26] S. Park and K. M. Mosalam, Simulation of Reinforced Concrete Frames with

[27] W.M. Hassan and J.Moehle, Quantification of residual axial capacity of beam-column joints in existing concrete buildings under seismic load reversals, *Compdyn 2013* – Kos Island, Greece, 12–14 June, 2013.

[28] Decreto Ministeriale n. 40 del 3/3/1975. Approvazione delle norme tecniche per le costruzioni in zone sismiche. G.U. n. 93 dell'8/4/1975. (in Italian)

[29] I. Iervolino, C. Galasso, E. Cosenza, REXEL: computer aided record selection for code-based seismic structural analysis, *Bulletin of Earthquake Engineering*, **8**(2), 339-362, 2010.

[30] O.C. Celik, and B.R. Ellingwood, Seismic fragilities for non-ductile reinforced concrete frames–Role of aleatoric and epistemic uncertainties, *Structural Safety*, **32**(1): 1-12, 2010.

[31] O.C. Celik. Probabilistic assessment of non-ductile reinforced concrete frames susceptible to Mid-America ground motions. PhD dissertation, School of Civil and Environmental Engineering, Georgia Institute of Technology, Atlanta, GA, 2007.

[32] D.Vamvatsikos, C.A. Cornell, Incremental dynamic analysis. *Earthquake Engineering and Structural Dynamics*, **31**(3), 491-514, 2002.

[33] N. Shome, C. A. Cornel, P. Bazzurro, J. E. Carballo, Earthquakes, records, and nonlinear responses. *Earthquake Spectra* (EERI); **14**(3):469–500, 1998.